Ngr. J. Multi. vol-2, issue-8 (Aug-2026) pp-434-444

ISSN: 3108-2750 (E), 3139-8065 (P)

Nexus Global Research Journal of Multidisciplinary

Journal Homepage: https://nexusglobalresearch.com/journal/ngrjm/

Research Article

# Experimental Assessment of Capital-Cost Reduction in a Helical Coiled-Tube Heat Exchanger Using Shell-Side Air-Bubble Injection

**Hiba Qasim Mohammed [1*]**

[1] *Kufa Institute, Department of mechanical Technologies, Al-Furat Al-Awsat Technical University, Al-Najaf, Iraq*

**ABSTRACT:**
Integrating air bubbles into the liquid phase of thermal exchangers serves as an efficient active strategy for improving convective heat transfer. This research examines the possibility of decreasing capital costs by incorporating tiny bubbles onto a Vertical - shell's shell side -and-helical-coiled-cylindrical thermal exchanger through a porous sparger. The thermal efficiency was assessed by altering the water flow rates on the shell side, the air injection flow rates, and the fluctuations in intake temperature. The comprehensive thermal transfer coefficient was determined by the experimental energy balancing and the logarithmic average temp discrepancy, whereas the thermal transfer area scaling, according to the six-tenths rule, was employed to forecast the cost trajectory. Bubbling raised the total coefficient appreciably, with a maximum enhancement of approximately 119%. At a fixed heat duty, this implies a thermal transfer-area reduction of approximately 54.3% and, under the six-tenths rule, a predicted capital-cost reduction of approximately 37.5%. Shell-side bubbling therefore appears able to improve the economics of compact coiled-tube exchangers. The conclusion is conditional, however: compressor cost, air-injection power, pumping power, maintenance, and long-term reliability were left out of the present cost estimate.

**Keywords:** Helical coiled-cylindrical thermal exchanger; air-bubble injection; porous sparger; total coefficient of thermal transfer; capital-cost estimation; thermal transfer enhancement

**Citation:** Mohammed, H. Q. (2026). Experimental assessment of capital-cost reduction in a helical coiled-tube heat exchanger using shell-side air-bubble injection. Nexus Global Research Journal of Multidisciplinary, 2(8), 434–444.

## 1. INTRODUCTION:

Thermal exchangers appear throughout thermal systems, process plants, refrigeration equipment, energy-recovery units, and chemical processing, and in many installations, they represent a large share of the capital cost. A modest gain in heat transfer can thus shrink the surface area required, save material, and lower equipment cost — which is why enhancement remains central to the design and optimisation of both compact and conventional exchangers [1]–[3].

Enhancement techniques fall into passive, active, and compound groups. Passive schemes rely on geometry, inserts, extended surfaces, or secondary-flow generation, whereas active schemes call for an external input that disturbs the thermal or hydrodynamic boundary layers. Bubble injection is an active method, a dispersed gas phase is added to the liquid and, if the bubbles are carefully controlled, the resulting bubble motion increases local mixing, degrades the thermal boundary layer and increases turbulence in the vicinity of the heat transfer surface. [4]–[6].

How well the method performs depends on bubble size, air-flow rate, injector design, flow orientation, and the local hydrodynamics. Small, sub-millimetre bubbles tend to promote stronger mixing while limiting the insulating effect that large gas pockets can introduce [6], [7]. Earlier work has reported gains in the thermal transfer coefficient, Nusselt number, number of transfer units, and effectiveness for vertical and horizontal shell-and-coiled-tube exchangers [8]–[15]. Broader studies of bubbly flow likewise confirm that bubble-induced agitation reshapes heat transport by amplifying velocity fluctuations and disturbing near-wall transfer [16].

The thermal benefit of bubbling has been documented at length, yet its cost consequence is examined far less often. Since exchanger capital cost is tied closely to thermal transfer area, a higher total coefficient can lower the area needed for a given

***Corresponding Author:** Hiba Qasim Mohammed, Email: hiba.mohammed@atu.edu.iq

**Received:** 05 Aug 2026 | **Accepted:** 13 Aug 2026 | **Published:** 17 Aug 2026

duty, and that area saving can in turn be translated into a preliminary cost reduction through established costing and scale-up correlations [17]–[25].

This link is assessed here for a Vertical - shell-and-helical-coiled-tube exchanger with air admitted on the shell side. Fine bubbles were generated by a porous sparger, thermal performance was measured, and the associated cost trend was inferred from the interplay of thermal transfer area, total coefficient, and cost scale-up. The study poses a practical design question: can the measured thermal gain from bubbling be carried through into a meaningful cut in exchanger capital cost?

## 2. UNCERTAINTY ANALYSIS:

The reliability of the measured and computed quantities was assessed using an uncertainty analysis. The root-sum-square propagation method was used to calculate the total uncertainty for a result R that relies on several independent measured variables *xi*. [18]:

$$W_R = \left[\left(\frac{\partial R}{\partial x_1}W_1\right)^2 + \left(\frac{\partial R}{\partial x_2}W_2\right)^2 + \cdots + \left(\frac{\partial R}{\partial x_n}W_n\right)^2\right]^{1/2}$$

Uncertainties in the calculated parameters followed from those in the measured flow rates, temperatures, and derived thermal quantities. For the total coefficient, contributions came from the measured mass-flow rates, specific heat, stream temperature differences, and thermal transfer area. Temperature errors propagated into both the heat duty and the log-average temp discrepancy, while flow-rate errors entered the heat duty. Because the predicted capital cost was derived from the total coefficient through the area–cost relation, it was assigned the same relative uncertainty. Rather than evaluating each sensitivity coefficient term by term, the combined uncertainties listed in Table 1 were adopted. The water and air rotameters were accurate to approximately ±2% and ±2.5%, respectively, and temperature readings to ±0.4 °C. The combined uncertainties of the total coefficient and predicted cost are dominated by the temperature-difference terms. Table 1 summarises the main instrument uncertainties and the resulting uncertainties in the calculated quantities.

**Table 1. Uncertainty of the instruments and the calculated performance parameters.**

| Parameter | Uncertainty |
|---|---|
| Water flow-rate measurement accuracy | ±2% |
| Air flow-rate measurement accuracy | ±2.5% |
| Hot-fluid inlet temp (°C) | ±0.4 |
| Hot-fluid outlet temp (°C) | ±0.4 |
| Cold-fluid intake temp (°C) | ±0.4 |
| Cold-fluid outlet temp (°C) | ±0.4 |
| Cold-fluid columns temp T1 (°C) | ±0.4 |
| Cold-fluid columns temp T2 (°C) | ±0.4 |
| Cold-fluid columns temp T3 (°C) | ±0.4 |
| Cold-fluid columns temp T4 (°C) | ±0.4 |
| Air inlet temp (°C) | ±0.4 |
| Air outlet temp (°C) | ±0.4 |
| Total coefficient of thermal transfer | ±15.80% |
| Capital cost | ±15.80% |

## 3. EXPERIMENTAL SETTING AND PROCEDURE

### 3.1 Experimental Setting

The apparatus consisted of a bubble generating system, a data acquisition system, a test exchanger, a heating unit, and a cooling unit. The water on the shell side originated from a chilled water reservoir equipped with a refrigeration system, whilst the hot water for the coil was sourced from a heated storage tank using electric heaters and a wattmeter. A compressor for aquariums supplied oxygenated air to the permeable sparger. The introduced bubbles ascended towards the cold water, However, the hot water flowed in the opposite direction from the cold water on the shell side.

In an effort to mitigate thermal dissipation, the cold water reservoir, the hot water reservoir, and the testing zone were each insulated. K-type thermocouples were employed to record the inlet, exit, and specific shell-side temperatures, which were connected to a PICOLOG TC-08 data recorder. Calibrated rotameters were employed to evaluate the flow rates of air and water, while a digital manometer was employed to monitor the pressure differential. Figure 1 illustrates the configuration.

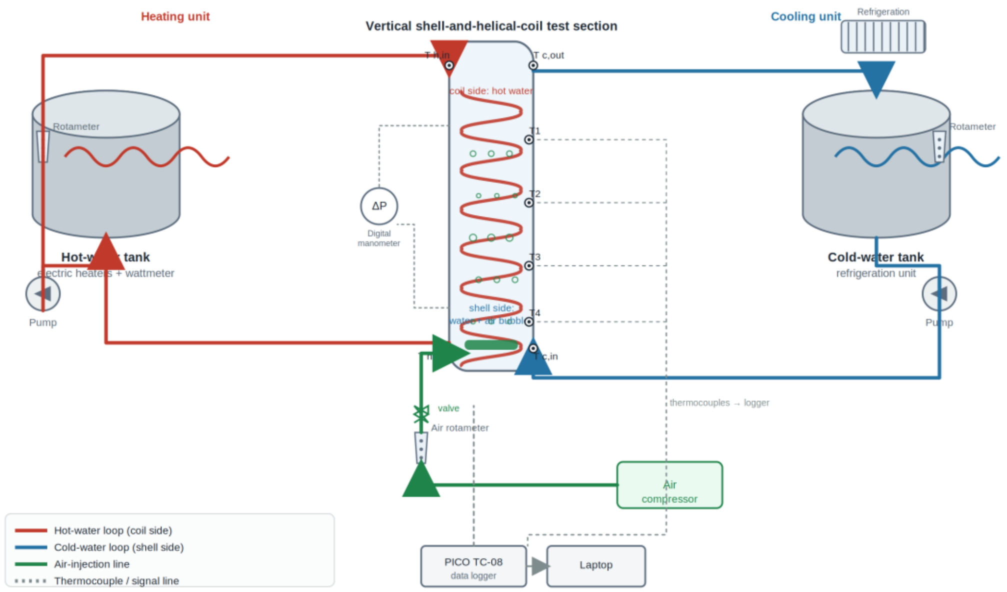


**Figure 1. Schematic representation of the experimental configuration employed for air-bubble injection in the shell side of the helical coiled-cylindrical thermal exchanger.**

Table 2 lists the essential geometric characteristics of the coiled tube and the shell. The shell measured 500 mm in height and possessed an internal diameter of 152.4 mm. The uncoiled length of the coiled tube was 3939 mm, featuring an inner diameter of 4.4 mm, a wall thickness of 1.6 mm, an average coil diameter of 114 mm, comprising 11 turns, and a pitch of 30 mm. The arrangement of the coil and the resulting length are equivalent, since NπD_c=11×π×114≈3939 mm.

**Table 2. Geometrical specifications of the shell and the coiled tube.**

| **Component** | **$D_i$ (mm)** | **t (mm)** | **H (mm)** | **L (mm)** | **$D_c$ (mm)** | **$d_i$ (mm)** | **N** | **P (mm)** |
|---|---|---|---|---|---|---|---|---|
| Shell | 152.4 | 3 | 500 | – | – | – | – | – |
| Coiled tube | – | 1.6 | 380 | 3939 | 114 | 4.4 | 11 | 30 |

### 3.2 Experimental Method:

A broad envelope of operating conditions was covered. Three inlet temp differences between the hot coil side and the cold shell side were tested — 20 °C, 30 °C, and 36 °C. At each temperature difference, the coil-side water flow rate was fixed in turn at 1.0, 1.5, and 2.0 L/min; the shell-side water flow rate was swept from 2 to 10 L/min; and the air-flow rate was swept from 0 to 10 L/min, with the zero-air condition serving as the reference. Readings were taken only after steady-state conditions had been reached. Table 3 sets out the matrix for the first experimental set (ΔT = 20 °C), and the same matrix was applied for the ΔT = 30 °C and 36 °C cases.

**Table 3. Test-condition matrix for the first experimental set (ΔT = 20 °C).**

| Coil-side water flow rate (L/min) | Shell-side water flow rate (L/min) | Air flow rate (L/min) |
|---|---|---|
| 1.0 | 2 | 0, 2, 4, 6, 8, 10 |
| 1.0 | 4 | 0, 2, 4, 6, 8, 10 |
| 1.0 | 6 | 0, 2, 4, 6, 8, 10 |
| 1.0 | 8 | 0, 2, 4, 6, 8, 10 |
| 1.0 | 10 | 0, 2, 4, 6, 8, 10 |
| 1.5 | 2 | 0, 2, 4, 6, 8, 10 |
| 1.5 | 4 | 0, 2, 4, 6, 8, 10 |
| 1.5 | 6 | 0, 2, 4, 6, 8, 10 |
| 1.5 | 8 | 0, 2, 4, 6, 8, 10 |
| 1.5 | 10 | 0, 2, 4, 6, 8, 10 |
| 2.0 | 2 | 0, 2, 4, 6, 8, 10 |
| 2.0 | 4 | 0, 2, 4, 6, 8, 10 |
| 2.0 | 6 | 0, 2, 4, 6, 8, 10 |
| 2.0 | 8 | 0, 2, 4, 6, 8, 10 |
| 2.0 | 10 | 0, 2, 4, 6, 8, 10 |

### 3.3 Data Reduction

The primary measure of thermal performance was chosen to be the total coefficient of thermal transfer, or $U$. It was derived using the log-average temp discrepancy, the heat duty, and the thermal transfer area. [17], [26]:

$$U = \frac{q}{A_s\,\Delta T_{LMTD}}$$

where q denotes the rate of heat transfer, A_s represents the surface area for heat transfer, and ΔTLMTD signifies the log-mean temperature differential. The thermal transfer rate was determined using the energy balance between the hot and cold streams:

$$q = \dot{m}_h c_{p,h}\left(T_{h,i} - T_{h,o}\right) = \dot{m}_c c_{p,c}\left(T_{c,o} - T_{c,i}\right)$$

The log-average temp discrepancy for counter-flow operation was evaluated as:

$$\Delta T_{LMTD} = \frac{\left(T_{h,i} - T_{c,o}\right) - \left(T_{h,o} - T_{c,i}\right)}{\ln\left[\left(T_{h,i} - T_{c,o}\right)/\left(T_{h,o} - T_{c,i}\right)\right]}$$

The cost analysis was based on the relationship between the thermal transfer area and the heat-exchanger capital cost. Because the required area decreases as $U$ increases for a fixed heat duty and temperature driving force, the ratio of capital costs between the reference and the enhanced cases was related to the ratio of their thermal transfer areas through the six-tenths rule, which is commonly used for preliminary equipment-cost estimation [22]–[25]:

$$\frac{C_A}{C_B} = \left(\frac{A_A}{A_B}\right)^{0.6}$$

Combining the area relation with the overall thermal transfer equation made it possible to estimate, relative to the no-air reference, the cost reduction produced by bubbling. This area–cost scaling follows standard heat-exchanger design and process-economics practice [27]–[29].

## 4. DISCUSSION AND RESULTS:

### 4.1 Total coefficient of thermal transfer

Figure 2 traces the total coefficient against Flow rates on the shell side for the various air-flow rates and inlet temp differences. In every case, shell-side bubbling raised the coefficient above the no-air reference. The gain is attributed to the rising bubbles, which stir the liquid, break up the thermal boundary layer around the coiled tube, and sharpen mixing near the thermal transfer surface.

The coefficient also climbed as the Flow rates on the shell side rose — as expected, since a faster liquid stream thins the thermal boundary layer and aids convection. Injection was more effective at higher air-flow rates, though the gain flattened towards the top of the tested range, where extra bubbles contributed progressively less near-wall mixing. Over the conditions examined, the largest enhancement was approximately 119%.

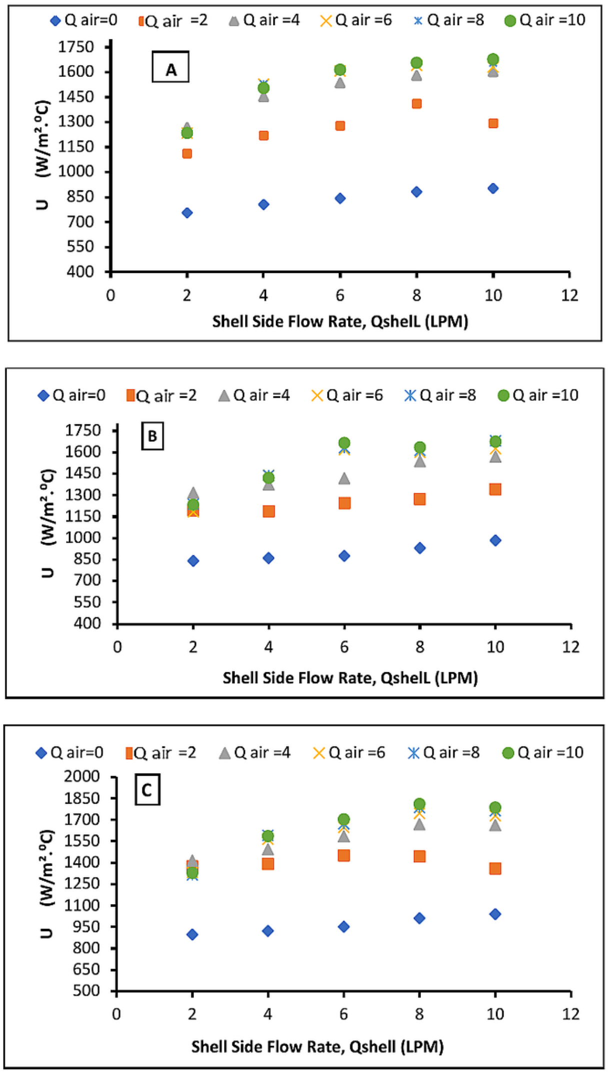


**Figure 2: Effect of air-bubble injection on the total coefficient of thermal transfer at Q_coil = 1 L/min: (a) ΔT = 20 °C, (b) ΔT = 30 °C, and (c) ΔT = 36 °C.**

**4.2 Capital-Cost Prediction:**

The gain in the total coefficient was then carried into a predicted cost reduction. At a fixed heat duty and temperature driving force, a higher coefficient calls for a smaller thermal transfer area; and because exchanger cost is usually tied to area through a power law, the smaller area yields a lower estimated cost. Compressor purchase, air-injection power, and the extra pumping demand were not counted. The outcome should therefore be read as a cost prediction for the exchanger body, not as a full life-cycle assessment.

Figure 3 plots the predicted cost index against Flow rates on the shell side for the no-air and air cases. The index fell as the Flow rates on the shell side rose, because the required area shrank, and bubbling lowered it further still relative to the no-air reference. At the peak coefficient enhancement of approximately 119% (U ratio ≈ 2.19), the thermal transfer area fell by approximately 54.3%; applying the six-tenths rule to that saving gave a predicted maximum capital-cost reduction of approximately 37.5%. A linear area–cost relation (exponent 1.0) would set the cost reduction equal to the area reduction (≈54.3%), a case kept only for the sensitivity study in Section 4.3. Bubble-assisted enhancement thus offers a possible economic advantage, provided the auxiliary equipment and its running costs stay modest.

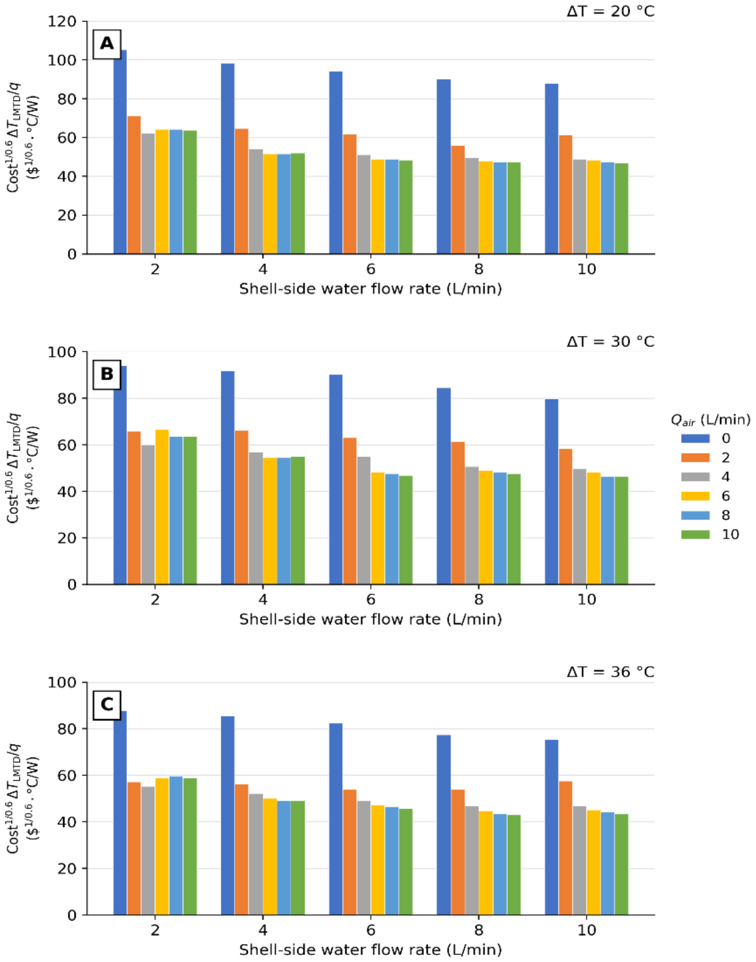


**Figure 3: Variation of the predicted heat-exchanger cost index with Flow rates on the shell side at Q_coil = 1 L/min: (a) ΔT = 20 °C, (b) ΔT = 30 °C, and (c) ΔT = 36 °C.**

### 4.3 Sensitivity of the Predicted Cost Reduction to the Cost-Scaling Exponent:

The predicted capital-cost reduction depends on the exponent adopted in the area–cost scaling law. For a fixed heat duty and temperature driving force, the required area scales inversely with the total coefficient of thermal transfer, so the ratio of the enhanced-to-reference area is $A_{air}/A_{no-air} = U_{no-air}/U_{air}$. For the maximum measured enhancement of approximately 119% (i.e. $U_{air}/U_{no-air} \approx 2.19$), the predicted cost reduction was evaluated as $R = 1 - (A_{air}/A_{no-air})^n$ for cost-scaling exponents $n$ between 0.6 and 1.0, with the six-tenths rule ($n = 0.6$) taken as the base case. The resulting sensitivity is presented in Table 4.

**Table 4. Sensitivity of the predicted maximum capital-cost reduction to the area–cost scaling exponent, evaluated at the maximum measured overall-coefficient enhancement (~119%, U ratio ≈ 2.19). Values are an analytical assessment, not new experimental data.**

| Cost-scaling exponent, n | Basis | Predicted maximum cost reduction (%) |
|---|---|---|
| 0.6 | Six-tenths rule (adopted base case) | 37.5 |
| 0.7 | Intermediate | 42.2 |
| 0.8 | Intermediate | 46.6 |
| 0.9 | Intermediate | 50.6 |
| 1.0 | Linear area–cost relation (= area reduction) | 54.3 |

With the six-tenths rule as the base case, the predicted maximum capital-cost reduction is approximately 37.5%. The maximum thermal transfer-area reduction is approximately 54.3%; a cost reduction of that same size would arise only under a linear area–cost relation (n = 1.0), which is retained as a sensitivity case rather than as the main cost result.

### 4.4 Net Techno-Economic Considerations:

The saving described above concerns only the exchanger body and the thermal transfer-area effect. A complete assessment would weigh this capital saving against the auxiliary air-injection system and the added operating energy. A first-order framework may be written as

$$\Delta C_{net} = \Delta C_{capital} - \left(C_{comp} + C_{energy}\right)$$

where $\Delta C_{capital}$ is the area-based capital saving, $C_{comp}$ is the purchase cost of the air compressor and distribution hardware, and $C_{energy}$ is the capitalised cost of the additional operating energy over the design life. The operating-energy term combines the air-injection power and the incremental pumping power required to overcome any added shell-side resistance:

$$P_{op} = P_{air} + P_{pump} = \frac{\dot{V}_{air}\,\Delta p_{sparger}}{\eta_{comp}} + \frac{\dot{V}_{water}\,\Delta p_{shell}}{\eta_{pump}}$$

Compressor power, pumping power, sparger pressure drop, shell-side pressure drop, component efficiencies, and annual operating hours were not measured in this study and should be established in future work. The reported figure is accordingly a capital-cost prediction for the exchanger body rather than a net or life-cycle saving; once compressor cost and operating energy are folded in, the net benefit will be smaller.

### 4.5 Benchmarking Against Previous Air-Injection Studies

Table 5 sets the present work against representative experimental studies of air injection in shell-and-coil and related thermal exchangers. The thermal gain measured here falls within the range those studies report. What sets this work apart is that the thermal gain is carried through to a capital-cost prediction — a step the earlier studies listed in Table 5 did not take.

**Table 5. Comparison of the present study with previous air-bubble-injection thermal transfer studies.**

| Study | Heat-exchanger configuration | Primary analysis focus | Economic (capital-cost) analysis |
|---|---|---|---|
| Present study | Vertical - shell-and-helical-coil | Thermal transfer enhancement and capital-cost prediction | Yes |
| Sadighi Dizaji et al. [8] | Vertical - shell-and-coil | Exergy and NTU analysis | No |
| Panahi [9] | Vertical - shell-and-coil | Nusselt number and effectiveness | No |
| Khorasani & Dadvand [10] | Horizontal helical shell-and-coil | Thermal transfer performance | No |
| El-Said & Alsood [11] | Horizontal shell-and-multitube (baffled) | Thermal transfer performance | No |
| Khorasani et al. [12] | Shell-and-coiled tube (coil-side injection) | Second-law (exergy) analysis | No |
| Baqir et al. [13] | Vertical - shell-and-helical-coil | NTU and effectiveness | No |
| Sokhal et al. [14] | Shell-and-tube | Heat transfer and exergy loss | No |
| Ghashim & Flayh [15] | Shell-and-tube (helical coil) | Thermal transfer enhancement and pressure drop | No |

### 4.6 Limitations

When analysing the results, keep the following constraints in mind:

- Only the thermal transfer-area effect entered the capital-cost analysis; the compressor capital cost and the air-distribution hardware were excluded.
- Compressor operating energy and the incremental pumping power were left out, so the reported value is a capital-cost prediction rather than a net saving.
- The shell-side pressure drop and its pumping penalty were not quantified. A digital manometer was installed, but the pressure-drop data were not reported and should be measured in future work.
- The economic result is not a full life-cycle cost analysis. Compressor purchase, maintenance, fouling, and annual operating hours would all be required for that assessment.
- The predicted cost reduction depends on the assumed area–cost scaling exponent (Section 4.3) and on the selected cost model.

The technique is thus best suited when thermal gain is high and the extra cost and energy use of the auxiliary system is not that significant. The method should only be recommended after a complete cost-based analysis of capital and operating costs have been conducted.

## 5. CONCLUSIONS:

This work assessed experimentally how shell-side bubbling affects the thermal performance and predicted capital cost of a Vertical - shell-and-helical-coiled-cylindrical thermal exchanger. Fine bubbles were produced by a porous sparger, and the tests covered several water-flow rates, air-flow rates, and inlet temp differences. The main conclusions are as follows:

- Bubbling raised the total coefficient of thermal transfer above the no-air reference, an improvement traced to bubble-induced mixing, boundary-layer disruption, and stronger turbulence in the shell-side liquid. The maximum enhancement reached approximately 119% under the tested conditions.
- That approximately 119% peak enhancement corresponds to a thermal transfer-area reduction of approximately 54.3%. Under the six-tenths rule, this area reduction gives a predicted

maximum capital-cost reduction of approximately 37.5%.

- The sensitivity analysis showed the predicted cost reduction to hinge on the area–cost exponent: approximately 37.5% under the adopted six-tenths rule, rising to the area-reduction value (≈54.3%) only under a linear relation. A net techno-economic framework was also outlined for future completion once compressor and pumping-power data become available.
- Cost of compressor, air-injection power, variation in pumping power and maintenance requirements were beyond the scope of the present calculation. Therefore, a full techno-economic study is required prior to the application of the method for industrial design.

**Nomenclature:**

**Table 6. Nomenclature.**

| Symbol | Definition | Unit |
|---|---|---|
| $A_s$ | Thermal transfer surface area | m² |
| C | Heat-capacity rate (ṁ·c_p) | W/K |
| $c_p$ | Specific heat | J/kg·K |
| $D_c$ | Mean coil diameter | m |
| $d_i$ | Tube inner diameter | m |
| H | Height | m |
| k | Thermal conductivity | W/m·K |
| L | Tube (developed) length | m |
| ṁ | Mass-flow rate | kg/s |
| N | Number of coil turns | – |
| Nu | Nusselt number | – |
| P | Coil pitch | m |
| q | Thermal transfer rate | W |
| Q | Volumetric flow rate | L/min |
| T | Temperature | °C or K |
| U | Total coefficient of thermal transfer | W/m²·K |
| W | Measurement uncertainty | – |
| $\Delta T_{LMTD}$ | Log-average temp discrepancy | °C or K |

## REFERENCES:

[1] A. E. Bergles, “ExHFT for fourth generation heat transfer technology,” *Experimental Thermal and Fluid Science*, vol. 26, no. 2–4, pp. 335–344, 2002.

[2] R. L. Webb and N.-H. Kim, *Principles of Enhanced Heat Transfer*, 2nd ed. New York: Taylor & Francis, 2005.

[3] R. K. Shah and D. P. Sekulic, *Fundamentals of Heat Exchanger Design*. Hoboken, NJ: Wiley, 2003.

[4] S. H. Sadighi Dizaji, “Heat transfer enhancement due to air bubble injection into a horizontal double-pipe heat exchanger,” *International Journal of Automotive Engineering*, vol. 4, no. 4, pp. 973–980, 2015.

[5] A. Moosavi, M. Abbasalizadeh, and H. Sadighi Dizaji, “Optimization of heat transfer and pressure drop characteristics via air bubble injection inside a shell and coiled cylindrical thermal exchanger,” *Experimental Thermal and Fluid Science*, vol. 78, pp. 1–9, 2016.

[6] A. Kitagawa, K. Kosuge, K. Uchida, and Y. Hagiwara, “Heat transfer enhancement for laminar natural convection along a vertical plate due to sub-

millimeter-bubble injection," *Experiments in Fluids*, vol. 45, no. 3, pp. 473–484, 2008.

[7] A. Kitagawa and Y. Murai, "Pulsatory rise of microbubble swarm along a vertical wall," *Chemical Engineering Science*, vol. 116, pp. 694–703, 2014.

[8] H. Sadighi Dizaji, S. Jafarmadar, M. Abbasalizadeh, and S. Khorasani, "Experiments on air bubbles injection into a Vertical - shell and coiled cylindrical thermal exchanger: exergy and NTU analysis," *Energy Conversion and Management*, vol. 103, pp. 973–980, 2015.

[9] D. Panahi, "Evaluation of Nusselt number and effectiveness for a Vertical - shell-coiled cylindrical thermal exchanger with air bubble injection into the shell side," *Experimental Heat Transfer*, vol. 30, no. 3, pp. 179–191, 2017.

[10] S. Khorasani and A. Dadvand, "Effect of air bubble injection on the performance of a horizontal helical shell and coiled cylindrical thermal exchanger: an experimental study," *Applied Thermal Engineering*, vol. 111, pp. 676–683, 2017.

[11] E. M. S. El-Said and M. M. A. Alsood, "Experimental investigation of air injection effect on the performance of a horizontal shell and multi-cylindrical thermal exchanger with baffles," *Applied Thermal Engineering*, vol. 134, pp. 238–247, 2018.

[12] M. Saleh Khorasani, A. Moosavi, and A. Dadvand, "A comprehensive second-law analysis of coil-side air injection in the shell and coiled cylindrical thermal exchanger: an experimental study," *Applied Thermal Engineering*, vol. 150, pp. 80–87, 2019.

[13] A. S. Baqir, H. B. Mahood, and A. R. Kareem, "Optimization and evaluation of NTU and effectiveness of a helical coil cylindrical thermal exchanger with air injection," *Thermal Science and Engineering Progress*, vol. 14, Art. 100420, 2019.

[14] G. S. Sokhal, G. S. Dhindsa, K. S. Sokhal, M. Ghazvini, M. Sharifpur, and M. Sadeghzadeh, "Experimental investigation of heat transfer and exergy loss in a heat exchanger with an air-bubble injection technique," *Journal of Thermal Analysis and Calorimetry*, vol. 145, no. 3, pp. 727–737, 2021. doi: 10.1007/s10973-020-10192-1.

[15] S. L. Ghashim and A. M. Flayh, "Experimental investigation of heat transfer enhancement in a heat exchanger due to air-bubble injection," *Journal of King Saud University – Engineering Sciences*, vol. 33, no. 7, pp. 517–524, 2021. doi: 10.1016/j.jksues.2020.06.006.

[16] B. Gvozdić, E. Alméras, V. Mathai, X. Zhu, D. P. M. van Gils, R. Verzicco, S. G. Huisman, C. Sun, and D. Lohse, "Experimental investigation of heat transport in homogeneous bubbly flow," *Journal of Fluid Mechanics*, vol. 845, pp. 226–244, 2018.

[17] T. L. Bergman, A. S. Lavine, F. P. Incropera, and D. P. DeWitt, *Fundamentals of Heat and Mass Transfer*, 7th ed. Hoboken, NJ: Wiley, 2011.

[18] J. P. Holman, *Experimental Methods for Engineers*, 8th ed. New York: McGraw-Hill, 2012.

[19] H. B. Mahood, A. N. Campbell, R. B. Thorpe, and A. O. Sharif, "Heat transfer efficiency and capital cost evaluation of a three-phase direct-contact heat exchanger for the utilisation of low-grade energy sources," *Energy Conversion and Management*, vol. 106, pp. 101–109, 2015.

[20] H. B. Mahood, *Experimental and Theoretical Investigation of a Three-Phase Direct-Contact Condenser*, Ph.D. dissertation, Dept. of Chemical and Process Engineering, University of Surrey, UK, 2016.

[21] G. Slavković, S. J. Budimir, I. M. Rakonjac, M. S. Jarić, and N. J. Budimir, "Techno-economic analysis of thermal exchangers with parallel helical tube coils," *Tehnički Vjesnik*, vol. 21, no. 4, pp. 861–866, 2014.

[22] D. S. Remer and L. H. Chai, "Process equipment, cost scale-up," in *Encyclopedia of Chemical Processing and Design*. New York: Marcel Dekker, 1993.

[23] M. S. Peters, K. D. Timmerhaus, and R. E. West, *Plant Design and Economics for Chemical Engineers*, 5th ed. New York: McGraw-Hill, 2003.

[24] R. Turton, R. C. Bailie, W. B. Whiting, J. A. Shaeiwitz, and D. Bhattacharyya, *Analysis, Synthesis, and Design of Chemical Processes*, 5th ed. Boston, MA: Prentice Hall, 2018.

[25] G. Towler and R. Sinnott, *Chemical Engineering Design: Principles, Practice and Economics of Plant and Process Design*, 2nd ed. Oxford, UK: Butterworth-Heinemann, 2013.

[26] S. Kakaç, H. Liu, and A. Pramuanjaroenkij, *Thermal exchangers: Selection, Rating, and Thermal Design*, 3rd ed. Boca Raton, FL: CRC Press, 2012.

[27] K. Thulukkanam, *Heat Exchanger Design Handbook*, 2nd ed. Boca Raton, FL: CRC Press, 2013.

[28] G. F. Hewitt, G. L. Shires, and T. R. Bott, *Process Heat Transfer*. Boca Raton, FL: CRC Press, 1994.

[29] R. Smith, *Chemical Process Design and Integration*, 2nd ed. Chichester, UK: Wiley, 2016.